Received 2 March 2021; accepted 14 March 2021. Date of publication 17 March 2021; date of current version 13 April 2021.
The review of this article was arranged by Editor C. C. McAndrew.

Digital Object Identifier 10.1109/JEDS.2021.3066811

Novel Low Loss LIGBT With Assisted Depletion N-Region and P-Buried Layer

LICHENG SUN, BAOXING DUAN, AND YINTANG YANG (Senior Member, IEEE)

Key Laboratory of the Ministry of Education for Wide Band-Gap Semiconductor Materials and Devices, School of Microelectronics, Xidian University, Xi'an 710071, China

CORRESPONDING AUTHOR: B. DUAN (e-mail: bxduan@163.com)

This work was supported in part by Science Foundation for Distinguished Young Scholars of Shaanxi Province under Grant 2018JC-017, and in part by 111 under Project B12026.

ABSTRACT A novel low loss lateral insulated gate bipolar transistor (LIGBT) with high voltage level is designed and studied in this paper, and is proposed with assisted depletion N-region (AD) and P-buried layer (PB) in the bulk Si substrate, named PBAD LIGBT. The proposed PBAD LIGBT utilizes the idea of electric field modulation (EFM) to greatly improve the breakdown voltage, which optimizes the lateral and longitudinal electric field distribution by introduced high electric field peak. Therefore, compared with conventional (Conv.) LIGBT, the shortened drift length of proposed PBAD LIGBT is beneficial to improve the forward and switching characteristics at the same time, while maintaining the same breakdown characteristics. When the breakdown voltage reaches 360 V, according to the TCAD simulation results, the drift length of proposed PBAD LIGBT is 20μm, which is 71.4% shorter than that of Conv. LIGBT of 70μm. As a result of shortening drift length, the forward voltage drop and turn-off loss of proposed PBAD LIGBT are reduced by 51.4% and 68.5%, respectively. The simulated trade-off curves show that, proposed PBAD LIGBT achieves significantly improved trade-off performance between turn-off loss and forward voltage drop than that of Conv. LIGBT, including PB LIGBT and AD LIGBT.

INDEX TERMS LIGBT, breakdown voltage, electric field modulation (EFM), turn-off loss, forward voltage drop.

I. INTRODUCTION

In silicon-based power semiconductor devices, lateral insulated gate bipolar transistors (LIGBT) have become the core device of energy conversion and transmission in power electronic system after more than 20 years of development [1], [2], which is mainly used in high-voltage DC power supply, smart grid and rail transportation [3]. Due to limitation of longitudinal electric field, conventional LIGBT with silicon-on-insulator (SOI) substrate is difficult to achieve very high breakdown voltage (BV) at the short drift length (L_D) condition [4]. Furthermore, the self-heating effect (SHE) introduced by SOI substrate will lead to many adverse effects, such as threshold voltage shift, deteriorating reliability and low carrier mobility [5]. To avoid the above problems, bulk Si substrate is developed to achieve higher BV, better heat dissipation and lower cost [6], [7].

Although LIGBT on bulk Si substrate are easier to achieve higher BV than that on SOI substrate, it also requires a large L_D to adapt higher voltage level applications. Due to the existence of conductivity modulation effect in drift region, the forward characteristics will not be greatly degraded. However, for the same condition, the switching characteristics will be greatly affected by more excess carriers.

The main method to reduce turn-off loss is to decrease turn-off time, which is to accelerate the removal process of excess carriers generated by forward conduction. One of commonly used structure to speed up the extraction of excess electrons is an anode-shorted (SA) design [8], which results in a negative differential resistance regime (NDR) in forward characteristic curves and further leads to possible oscillations during off-state. Separated shorted-anode (SSA) structure with the suppressed NDR [9] reduces the turn-off time while improves the working stability. However, because of the extended anode length of device, the large chip area is wasted and conductivity modulation in drift region is also weakened.

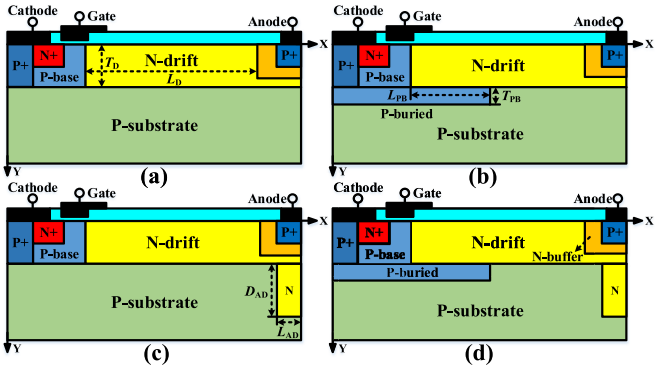

FIGURE 1. Schematic cross-section of (a) the Conv. LIGBT, (b) the PB LIGBT, (c) the AD LIGBT, and (d) the proposed PBAD LIGBT.

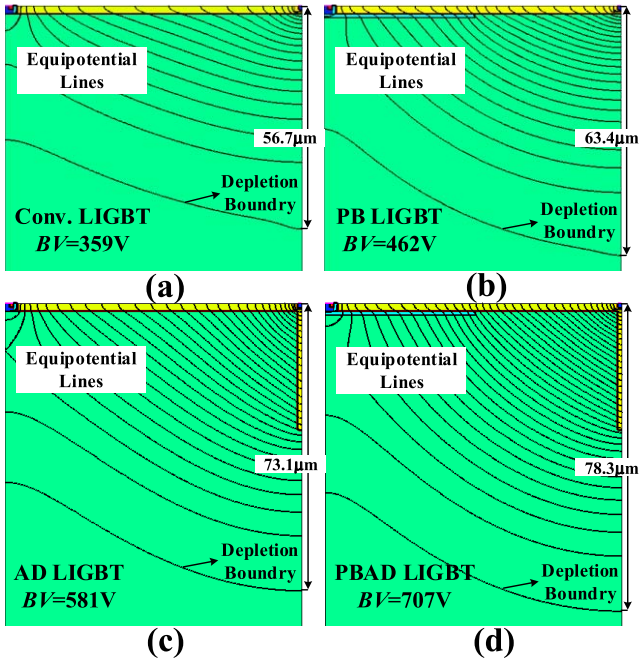

FIGURE 2. Simulated equipotential lines distribution (20V/line) of (a) the Conv. LIGBT, (b) the PB LIGBT, (c) the AD LIGBT, and (d) the proposed PBAD LIGBT at breakdown.

In addition, the shorter L_D makes it easier to achieve enhanced conductivity modulation and fewer excess carriers at the same time. Therefore, to meet the application requirements, the approach of improving BV instead of extending L_D can be used as another design way to reduce turn-off loss indirectly. References [10], [11] respectively report deep oxide trench formed in drift region of LDMOS and LIGBT that can reduce the device pitch to approximately the half of the conventional devices. Dual deep-oxide trenches (DDOTs) structure of [12] assists in sustaining the electric potential from anode, which also enables the shortening in device pitch. Reference [13] reports single-step buried oxide (SSBO) structure that modulates electric field distributions of drift region to gain high BV. Most of these structure designs require additional processing steps by forming oxide trenches or special buried oxide layer, which will further increase time and process costs.

In this paper, the proposed LIGBT makes full use of bulk Si substrate thickness to greatly improve BV, which achieves significantly improved trade-off performance between turn-off loss (E_{off}) and forward voltage drop (V_F). Although in view of the limitation of current standard CMOS process condition, for the great improvement of breakdown ability, the proposed structure is promising to meet the requirement of high voltage, high current and low turn-off loss in power electronic system.

II. DEVICE STRUCTURE

Fig. 1(d) shows the schematic cross-sectional view of the proposed LIGBT, which features assisted depletion N-region (AD) and P-buried layer (PB). The proposed PBAD LIGBT greatly improves BV by modulating the lateral and longitudinal electric field distribution with new high electric field peak. In addition, the PB LIGBT [14] in Fig. 1(b) shows that the PB structure is mainly optimized for the lateral electric field to make the distribution of surface electric field more uniform, and the AD LIGBT in Fig. 1(c) shows that the AD structure is mainly optimized for the longitudinal electric field to make the depletion of bulk Si substrate more sufficient. Meanwhile, the design of conventional (Conv.) LIGBT in Fig. 1(a) is based on the standard bulk Si technology without any extra introduced structures.

By satisfying RESURF concept [15] for lateral power devices, all LIGBT devices in Fig. 1 have adjusted the surface electric field distributions with optimized N_D to ensure the best breakdown ability. The doping concentration of P-substrate is 1.0×10^{14}cm^{-3}. The doping concentration of N-buffer and P-base is 1.0×10^{17} cm^{-3} and 5.0×10^{16} cm^{-3}, respectively. Both the PB and AD structure doping concentration are set as 5.0×10^{15} cm^{-3}. The device thickness (T_D) is 2μm, and N_D is the doping concentration of the N-drift while L_D and N_D vary with BV. In the proposed PBAD LIGBT, the PB structure length (L_{PB}) is half of L_D, T_{PB} is the thickness of PB structure, and the AD structure length (L_{AD}) is 1μm, D_{AD} is the depth of AD structure.

In this work, the physical models used in Sentaurus TCAD two-dimensional numerical simulation [16] include Mobility model (Doping DepHighFieldsat Enormal), EffectiveIntrinsic Density model (OldSlotboom), Recombination model (SRH (DopingDep) Auger Avalanche (Eparal)). And the criterion of device breakdown is set as BreakCriteria {Current (Contact = "drain" Absval = 1e-7)}.

III. RESULTS AND DISCUSSION

Fig. 2 shows the equipotential lines distribution for four types of LIGBT at breakdown. Highly doped PB structure can modulate the lateral electric field distribution, especially the surface electric field distribution, which makes the surface equipotential lines distribution denser. Furthermore, for Conv. LIGBT and PB LIGBT, the dense longitudinal equipotential lines at bottom of anode are easy to cause breakdown,

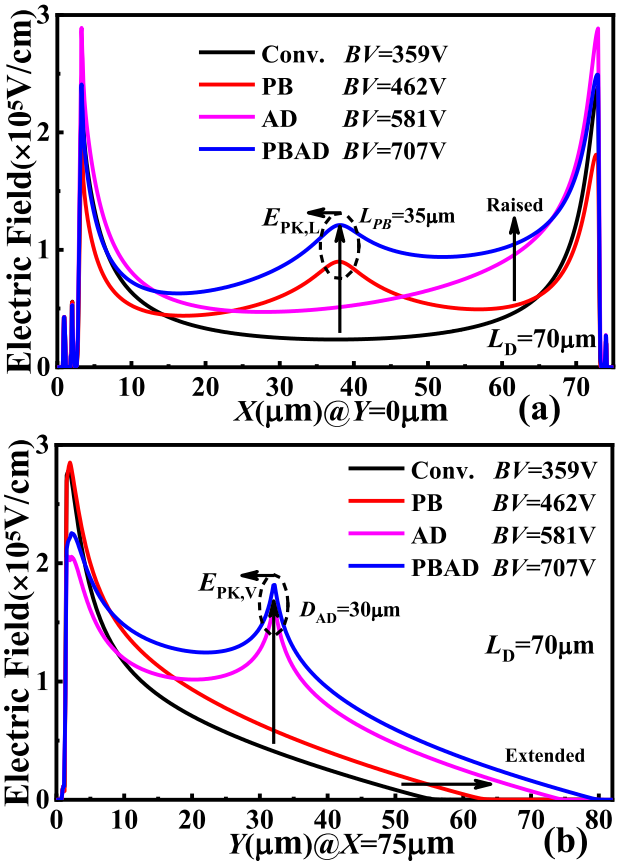

FIGURE 3. Simulated (a) surface and (b) longitudinal electric field distribution of the Conv. LIGBT, the PB LIGBT, the AD LIGBT, and the proposed PBAD LIGBT at breakdown.

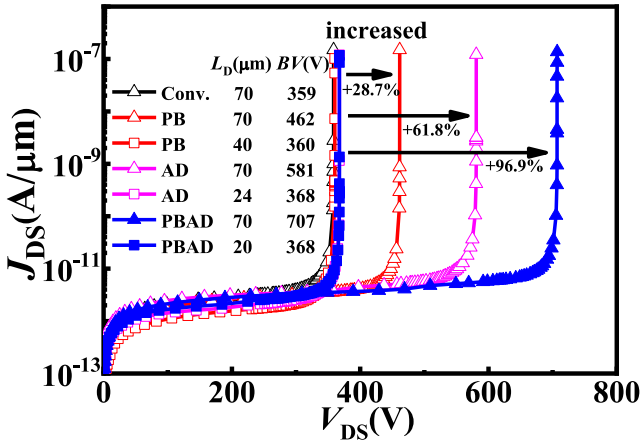

FIGURE 4. Simulated breakdown characteristic curves of the Conv. LIGBT, the PB LIGBT, the AD LIGBT, and the proposed PBAD LIGBT.

while the AD structure can sustain part of the electric field in substrate, so as to alleviate the peak electric field at anode bottom. Meanwhile, it can be clearly seen that the AD structure formed in the AD LIGBT and PBAD LIGBT makes the depletion boundary of longitudinal space charge region expand greatly, and the equipotential lines distribution are also more uniform, which realizes the full use of substrate thickness. The longitudinal depletion boundary depth of AD LIGBT (73.1μm) has been expanded by 28.9%, and that of PBAD LIGBT (78.3μm) has been expanded by 38.1%, respectively, compared with that of Conv. LIGBT (56.7μm).

Fig. 3 shows the surface and longitudinal electric field distribution for four types of LIGBT at breakdown. From the surface electric field distribution in Fig. 3(a), based on traditional U-shaped electric field curve, the PB structure produces additional electric field peak ($E_{PK,L}$) through electric field modulation (EFM) between highly doped buried layer and high impedance substrate. While through additional reversed PN junction formed by N-type region and substrate, the AD structure raises the whole electric field curve. Furthermore, from the longitudinal electric field distribution in Fig. 3(b), based on traditional triangle-shaped electric field curve, the PB structure raises and extends the whole electric field curve by EFM effect. While by additional reversed PN junction, the AD structure produces additional electric field peak ($E_{PK,V}$), alleviates the peak electric field at anode bottom and greatly extends the whole electric field curve. Due to the common optimization by EFM effect of PB and AD structure, the proposed PBAD LIGBT has more uniform lateral and longitudinal electric field distribution. Therefore, the BV of proposed PBAD LIGBT can reach 707V, which is improved by 96.9% than that of Conv. LIGBT (359V), 53.0% than that of PB LIGBT (462V), and 21.7% than that of AD LIGBT (581V), respectively.

Fig. 4 shows the breakdown characteristic curves for four types of LIGBT. Under the same $L_D = 70\mu m$, the BV of Conv. LIGBT is as lowest as 358V, while that of PB LIGBT, AD LIGBT and proposed PBAD LIGBT increases significantly and improves by 28.7%, 61.8% and 96.9%, respectively. Meanwhile, at the same BV level of 360V, the L_D of Conv. LIGBT is as largest as 70μm, while that of PB LIGBT (40μm), AD LIGBT (24μm) and proposed PBAD LIGBT (20μm) decreases significantly and reduces by 42.9%, 65.7% and 71.4%, respectively. Furthermore, the reverse leakage current of all devices is kept at a low value of about 10^{-12}A/μm. In order to satisfy the RESURF condition, the optimized N_D decreases with the decrease of L_D. As can be seen in Fig. 5, for the proposed PBAD LIGBT, the change trend of N_D is similar to that of AD LIGBT, while the initial higher N_D is similar to that of PB LIGBT. Finally, when $L_D = 20\mu m$, N_D can be obtained similar to that of Conv. LIGBT ($L_D = 70\mu m$), which is helpful to further optimize the forward characteristics.

Fig. 6 shows the forward I–V characteristic curves for four types of LIGBT. When the gate voltage $V_G = 10$V, V_F is the anode bias voltage at anode current density $J_{DS} = 100$A/cm^2. When the device starts to conduct, because the PB structure at cathode promotes the hole extraction process and weakens the conductivity modulation of drift region, the forward characteristics will be degraded. On the contrary, the AD structure promotes the electron accumulation at anode and enhances the conductivity modulation of drift region, so the

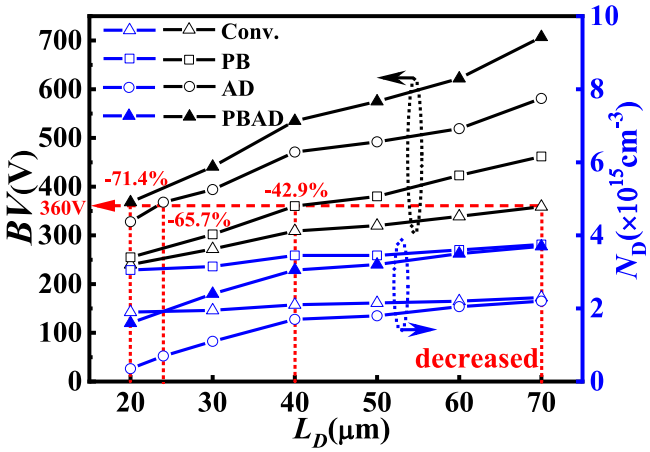

FIGURE 5. Simulated dependence of *BV* and N_D on the L_D for the Conv. LIGBT, the PB LIGBT, the AD LIGBT, and the proposed PBAD LIGBT.

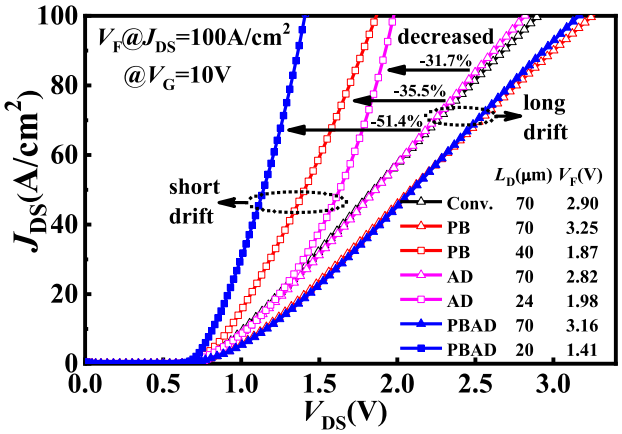

FIGURE 6. Simulated forward *I–V* characteristic curves of the Conv. LIGBT, the PB LIGBT, the AD LIGBT, and the proposed PBAD LIGBT.

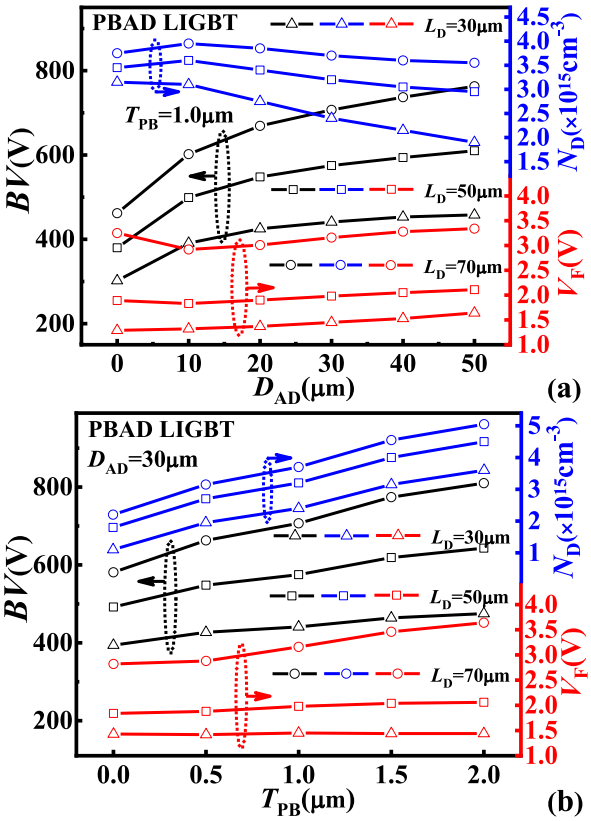

FIGURE 7. Simulated dependence of *BV*, V_F, and N_D on the (a) D_{AD} and (b) T_{PB} for the proposed PBAD LIGBT with different L_D.

forward characteristics will be improved. Therefore, compared to the V_F of Conv. LIGBT (2.90V) with the same device size, that of PB LIGBT (3.25V) is increased while that of AD LIGBT (2.82V) is decreased. However, considering the advantages of improved breakdown performance, it can be clearly seen in figure that the device with folded drift region has obtained lower V_F, that is, lower L_D can obtain better forward characteristics. For the same breakdown capability, the V_F of Conv. LIGBT is as highest as 2.90V, while that of PB LIGBT (1.87V), AD LIGBT (1.98V) and proposed PBAD LIGBT (1.41V) decreases significantly and reduces by 35.5%, 31.7% and 51.4%, respectively.

Fig. 7(a) compares the relationship between *BV*, V_F, N_D and D_{AD} for the proposed PBAD LIGBT with different L_D. With the increase of D_{AD}, the influence of AD structure on the surface peak electric field and longitudinal electric field distribution at anode increases gradually, and the *BV* increases accordingly. However, higher surface peak electric field needs lower N_D to maintain, which also makes V_F slowly improve. When $D_{AD} = 0\mu m$, that is, the situation that AD structure does not exist, but PB structure exists only, the forward characteristic is affected by the enhanced hole extraction, which will result in higher V_F, especially when L_D is high. Similarly, in Fig. 7(b), fixing D_{AD} and increasing T_{PB} means that the charge balance capability of PB structure in drift region is gradually enhanced, so *BV* and N_D also show a rising trend. In addition, thicker PB structure further enhances the hole extraction ability, which also leads to the improvement of V_F. The above results also show that with the increase of device size, *BV* will increase with the larger depletion area, N_D will increase by enhancing assisted depletion in substrate region, and V_F will increase due to the degradation of conductivity modulation in drift region.

Fig. 8 shows the switching characteristics curves with inductive load circuit for four types of LIGBT. The turn-off process of the device under inductive load can be divided into two stages. The first stage is the rise of anode bias voltage. At this time, V_{DS} increases while J_{DS} remains unchanged. The time spent in first stage (T_V) is related to the spreading speed of depletion region. According to Fig. 2, it can be seen that PB and AD structure has increased the substrate depletion area, so as that the time for V_{DS} to reach anode supply voltage will be longer. The voltage rise curves of devices with PB and AD structure in Fig. 8 also shows large capacitance effect, so the T_V of proposed PBAD LIGBT obtains the

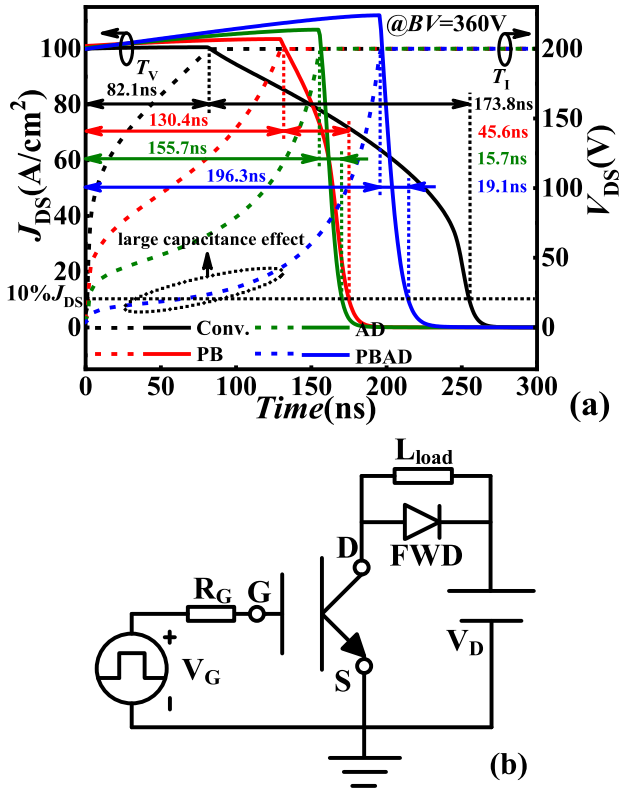

FIGURE 8. (a) Simulated switching characteristic curves with inductive load for the Conv. LIGBT, the PB LIGBT, the AD LIGBT, and the proposed PBAD LIGBT. (b) Schematic diagram of inductive load circuit for device switching simulation.

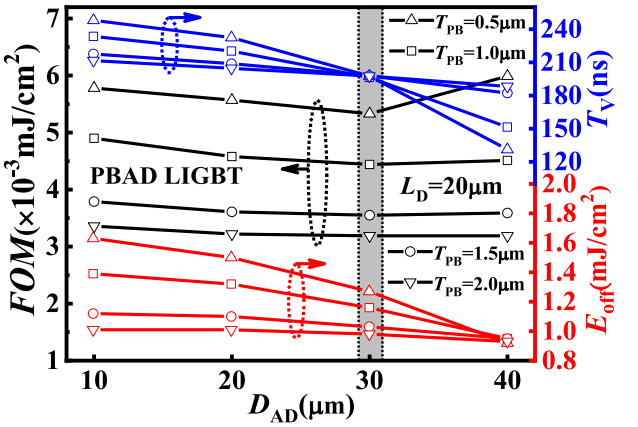

FIGURE 9. Simulated dependence of figure of merit (*FOM*), T_V, and E_{off} on the D_{AD} for the proposed PBAD LIGBT with different T_{PB}.

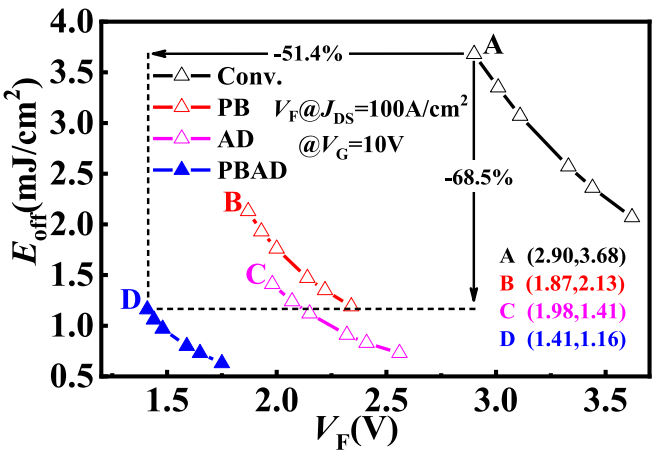

FIGURE 10. Simulated tradeoff curves of V_F versus E_{off} for the Conv. LIGBT, the PB LIGBT, the AD LIGBT, and the proposed PBAD LIGBT.

maximum value of 196.3ns. Similarly, the second stage is the drop of anode current. At this time, V_{DS} has reached anode supply voltage and remained unchanged while J_{DS} starts to decrease. The time spent in second stage (T_I) is mainly controlled by recombination speed of excess electron-hole pairs. Due to lower number of excess carriers in the folded drift region, the recombination process will be accelerated accordingly. The current drop curves of devices with folded drift region in Fig. 8 also show the alleviated current tailing, so the T_I of proposed PBAD LIGBT obtains the low value of 19.1ns. In the meantime, the value of E_{off} for devices can be obtained by the area integral formed through voltage rise curve and current drop curve. Therefore, it is shown from the figure that compared with Conv. LIGBT, the proposed PBAD LIGBT with the same high voltage capability can still obtain lower E_{off}.

Fig. 9 compares the relationship between figure of merit (*FOM*), T_V, E_{off} and D_{AD} for the proposed PBAD LIGBT with different T_{PB}. The special *FOM* here is defined as $FOM = (E_{\text{off}} \cdot V_{\text{F}})/BV$, which is used to characterize the trade-off performance between breakdown, forward and switching characteristics. And the smaller *FOM* is, showing that the larger denominator term is while the smaller numerator term is, so the better trade-off performance is. With the increase of T_{PB}, when D_{AD} is less than 30μm, T_V and E_{off} show a downward trend, while when D_{AD} is greater than 30μm, E_{off} presents a saturated state and T_V presents an opposite upward trend. The above curve changes can prove that when D_{AD}=30μm, the effect of AD structure on the device substrate is close to saturation. Finally, on the whole from figure, when D_{AD} = 30μm, the device can achieve the best trade-off performance, while maintaining low E_{off} and T_V.

By changing the doping concentration of the P-region at anode to control the hole injection efficiency of the device, the corresponding E_{off} can be obtained under different V_F values, so as to gain the trade-off curves of V_F versus E_{off} for four types of LIGBT in Fig. 10. The shortening of drift region has enhanced the conductivity modulation and reduced the number of excess carriers. Thus, compared to the Conv. LIGBT with the same breakdown capability, the V_F and E_{off} of proposed PBAD LIGBT is reduced by 51.4% and 68.5%, respectively. It can be proven that proposed PBAD LIGBT achieves significantly improved trade-off performance between E_{off} and V_F than Conv. LIGBT, including PB LIGBT and AD LIGBT.

The key fabrication process for the proposed PBAD LIGBT can be briefly described as follows: (1) Selecting P-type <100> epitaxial wafers with certain epitaxial thickness and high resistivity. (2) The masking layer is formed by chemical vapor deposition of SiN material, and the next step is to obtain assisted depletion region by deep reactive ion etching. (3) Formation of assisted depletion N-region by selective epitaxial growth technology. (4) Removing the masking layer and prepared highly doped P-buried layer by boron ion implantation annealing. (5) Epitaxial growth of new silicon layer. (6) The following process steps are consistent with the conventional LIGBT process, that is forming active region by ion implantation, gate oxide by dry oxidation, gate electrode by deposition and doping of polysilicon, and finally source and drain electrode by metal deposition, respectively.

IV. CONCLUSION

In summary, this paper reports a novel LIGBT structure with assisted depletion N-region and P-buried layer in the bulk Si substrate. By modulating the lateral and longitudinal electric field distribution with high electric field peak, the proposed PBAD LIGBT greatly shortens drift length from 70μm to 20μm while maintaining the high breakdown voltage of 360 V. As a result of shortening drift length, compared to Conv. LIGBT, the forward voltage drop and turn-off loss of proposed PBAD LIGBT is reduced by 51.4% and 68.5%, respectively, which achieves much lower turn-off loss and forward voltage drop at the same time. Therefore, fabricated in the standard CMOS process condition, the device with low cost bulk Si substrate is promising for high-frequency and high-power applications.

REFERENCES

[1] G. Amaratunga and F. Udrea, "Power devices for high voltage integrated circuits: New device and technology concepts," in *Proc. Int. Semicond. Conf. (CAS)*, vol. 2. Sinaia, Romania, 2001, pp. 441–448, doi: 10.1109/SMICND.2001.967503

[2] B. J. Baliga, *Fundamentals of Power Semiconductor Devices*. New York, NY, USA: Springer, 2008.

[3] B. J. Baliga, *The IGBT Device: Physics, Design and Applications of the Insulated Gate Bipolar Transistor*. Waltham, MA, USA: William Andrew, 2015.

[4] J.-P. Colinge, *Silicon-on-Insulator Technology: Materials to VLSI*. Boston, MA, USA: Kluwer Acad. Publ.,1991.

[5] M. A. Karim *et al.*, "Extraction of isothermal condition and thermal network in UTBB SOI MOSFETs," *IEEE Electron Device Lett.*, vol. 33, no. 9, pp. 1306–1308, Sep. 2012, doi: 10.1109/LED.2012.2205659.

[6] T. Trajkovic, N. Udugampola, V. Pathirana, G. Camuso, F. Udrea, and G. A. J. Amaratunga, "800V lateral IGBT in bulk Si for low power compact SMPS applications," in *Proc. 25th Int. Symp. Power Semicond. Devices IC's (ISPSD)*, Kanazawa, Japan, 2013, pp. 401–404, doi: 10.1109/ISPSD.2013.6694430.

[7] V. Pathirana, N. Udugampola, T. Trajkovic, and F. Udrea, "Low-loss 800-V lateral IGBT in bulk Si technology using a floating electrode," *IEEE Electron Device Lett.*, vol. 39, no. 6, pp. 866–868, Jun. 2018, doi: 10.1109/LED.2018.2831598.

[8] M. R. Simpson, "Analysis of negative differential resistance in the I-V characteristics of shorted-anode LIGBT's," *IEEE Trans. Electron Devices*, vol. 38, no. 7, pp. 1633–1640, Jul. 1991, doi: 10.1109/16.85160.

[9] D. S. Byeon, J. H. Chun, B. H. Lee, D. Y. Kim, M. K. Han, and Y. I. Choi, "The separated shorted-anode insulated gate bipolar transistor with the suppressed negative differential resistance regime," *Microelectron. J.*, vol. 30, no. 6, pp. 571–575, Jun. 1999, doi: 10.1016/S0026-2692(98)00180-3.

[10] H. Teranishi *et al.*, "A high density, low on-resistance 700V class trench offset drain LDMOSFET (TOD-LDMOS)," in *Proc. IEEE Int. Electron Devices Meeting*, Washington, DC, USA, 2003, pp. 1–4, doi: 10.1109/IEDM.2003.1269391.

[11] D. H. Lu, S. Jimbo, and N. Fujishima, "A low on-resistance high voltage soi ligbt with oxide trench in drift region and hole bypass gate configuration," in *IEEE Int. Electron Devices Meeting (IEDM) Tech. Dig.*, Washington, DC, USA, 2005, pp. 381–384, doi: 10.1109/IEDM.2005.1609356.

[12] L. Zhang *et al.*, "Low-loss SOI-LIGBT with dual deep-oxide trenches," *IEEE Trans. Electron Devices*, vol. 64, no. 8, pp. 3282–3286, Aug. 2017, doi: 10.1109/TED.2017.2712568.

[13] L. Sun, B. Duan, and Y. Yang, "Novel SOI LIGBT with fast-switching by the electric field modulation," *Micro Nano Lett.*, vol. 15, no. 3, pp. 155–158, Mar. 2020, doi: 10.1049/mnl.2019.0424.

[14] M. R. Simpson, P. A. Gough, F. I. Hshieh, and V. Rumennik, "Analysis of the lateral insulated gate transistor," in *Proc. Int. Electron Devices Meeting*, Washington, DC, USA, 1985, pp. 740–743, doi: 10.1109/IEDM.1985.191082.

[15] A. W. Ludikhuize, "A review of RESURF technology," in *Proc. 12th Int. Symp. Power Semicond. Devices ICs*, Toulouse, France, 2000, pp. 11–18, doi: 10.1109/ISPSD.2000.856763.

[16] *TCAD SentaurusDevice Manual*, Synopsys, Inc., Mountain View, CA, USA, 2013.